Atmospheric
Chemistry
and Physics

The Mediterranean summertime ozone maximum: global emission sensitivities and radiative impacts

N. A. D. Richards[1], S. R. Arnold[1], M. P. Chipperfield[1], G. Miles[2], A. Rap[1], R. Siddans[2], S. A. Monks[1], and M. J. Hollaway[1]

[1]Institute for Climate and Atmospheric Science, School of Earth and Environment, University of Leeds, LS2 9JT, Leeds, UK
[2]STFC Rutherford Appleton Laboratory, Harwell, Didcot, OX11 0QX, UK

Correspondence to: N. A. D. Richards (n.richards@see.leeds.ac.uk)

Abstract. The Mediterranean troposphere exhibits a marked and localised summertime ozone maximum, which has the potential to strongly impact regional air quality and radiative forcing. The Mediterranean region can be perturbed by long-range pollution import from Northern Europe, North America and Asia, in addition to local emissions, which may all contribute to regional ozone enhancements. We exploit ozone profile observations from the Tropospheric Emission Spectrometer (TES) and the Global Ozone Monitoring Experiment-2 (GOME-2) satellite instruments, and an offline 3-D global chemical transport model (TOMCAT) to investigate the geographical and vertical structure of the summertime tropospheric ozone maximum over the Mediterranean region. We show that both TES and GOME-2 are able to detect enhanced levels of ozone in the lower troposphere over the region during the summer. These observations, together with surface measurements, are used to evaluate the TOMCAT model's ability to capture the observed ozone enhancement. The model is used to quantify sensitivities of the ozone maximum to anthropogenic and natural volatile organic compound (VOC) emissions, anthropogenic NO_x emissions, wildfire emissions and long-range import of ozone and precursors. Our results show a dominant sensitivity to natural VOC emissions in the Mediterranean basin over anthropogenic VOC emissions. However, local anthropogenic NO_x emissions are result in the overall largest sensitivity in near-surface ozone. We also show that in the lower troposphere, global VOC emissions account for 40 % of the ozone sensitivity to VOC emissions in the region, whereas, for NO_x the ozone sensitivity to local sources is 9 times greater than that for global emissions at these altitudes. However, in the mid and upper troposphere ozone is most sensitive to non-local emission sources. In terms of radiative effects on regional climate, ozone contributions from non-local emission sources are more important, as these have a larger impact on ozone in the upper troposphere where its radiative effects are larger, with Asian monsoon outflow having the greatest impact. Our results allow improved understanding of the large-scale processes controlling air quality and climate in the region of the Mediterranean basin.

1 Introduction

Tropospheric ozone concentrations have increased since pre-industrial times, leading to a positive radiative forcing on climate (Forster et al., 2007b), and enhancement in ozone concentrations at the surface. Ozone at the surface is harmful to health (Levy et al., 2001; Gryparis et al., 2004; Ito et al., 2005), and damages vegetation, reducing crop yields (Fuhrer, 2009; Van Dingenen et al., 2009; Hollaway et al., 2012) and inhibits the terrestrial CO_2 sink (Sitch et al., 2007; Collins et al., 2010). Tropospheric ozone is produced in-situ through sunlight-initiated oxidation of volatile organic compounds (VOCs) in the presence of nitrogen oxides (NO_x) (Volz and Kley, 1988; Staehelin et al., 1994). Observations show that the Mediterranean troposphere exhibits a marked enhancement in summertime ozone, which maximises over the eastern basin (Butkovic et al., 1990; Varotsos and Cracknell, 1993; Kalabokas and Bartzis, 1998; Kalabokas et al., 2000, 2007; Kouvarakis et al., 2000, 2002; Lelieveld and Dentener, 2000; Kourtidis et al., 2002; Lelieveld et al., 2002; Roelofs

et al., 2003; Kalabokas and Repapis, 2004; Gerasopoulos et al., 2006; Castell et al., 2008). This feature is associated with anticyclonic conditions, subsidence, clear skies and high solar intensity, which enhances ozone photochemical production (Millan et al., 2002), and has the potential to strongly impact regional air quality and climate (Hauglustaine and Brasseur, 2001). This summertime antcyclonic flow results from Rossby wave response to the diabatic heating from convection in the Asian monsoon region, and produces descending air localized over the eastern Mediterranean and central Asia (Rodwell and Hoskins, 1996). Eastern Mediterranean tropospheric ozone column amounts are around 40–70 Dobson Units (DU) during summer (Kourtidis et al., 2002; Duncan et al., 2008) compared with around 20–30 DU units during winter. Summer (JJA) tropospheric ozone observations from the GOME satellite instrument suggest a seasonal-mean enhancement of $\sim$ 20 ppbv compared with other seasons in the region (Sauvage et al., 2007). Regional ozone background concentrations in the Eastern Mediterranean likely exceed the European Union (EU) 32 ppb over 24 h phytotoxicity limit year-round (Kourtidis et al., 2002). Gerasopoulos et al. (2006) found that 7-yr monthly average surface ozone measured in Crete (Eastern Mediterranean) exceeded 55 ppbv during the summer months, compared with less than 40 ppbv in winter. In the western Mediterranean basin, ozone enhancements have also been reported, with surface summertime average ozone concentrations at rural stations in Italy, eastern Spain, and Malta of more than 55–60 ppbv (Paoletti, 2006; Millan et al., 2000; Nolle et al., 2002), and up to 80 ppbv ozone has been observed by ship at the northern edge of the basin, close to the coasts of the south of France and northwest Italy during summer (Velchev et al., 2011). The prevalence of mountainous coastal topography leads to upslope winds during the daytime encouraging the formation of sea breeze circulation patterns (Millan et al., 1997). Upslope flow of surface air is linked to return flow aloft out over the sea, leading to a recirculation of pollutants, and creating stacked layers of pollution reaching 2–3 km in altitude, which undergo efficient photochemistry under intense solar insolation (Millan et al., 1997, 2000). During night, these air masses are held offshore by land breezes, creating reservoirs of aged pollution that are then brought onshore the following day (Gangoiti et al., 2001; Ancellet and Ravetta, 2005). Models and observations suggest that this local recirculation is of key importance for surface ozone in the Western Mediterranean (Jimenez et al., 2006; Velchev et al., 2011). Observations have also revealed the presence of well-preserved layers imported into the Western Mediterranean middle troposphere in long-range import from anthropogenic and forest fire emission sources in North America, with ozone concentrations of 75–90 ppbv, at least 50 % larger than 40–50 ppbv background tropospheric values (Ravetta et al., 2007).

Recent work has highlighted the role of the import of ozone-rich air masses from the upper-troposphere lower-stratosphere (UTLS) in enhancing summertime tropospheric ozone. Large-scale subsidence associated with anti-cyclonic conditions result in enhanced ozone in the lower troposphere and to the boundary layer over the Eastern Mediterranean (Kalabokas et al., 2013). The same phenomenon has been deduced from ship-borne ozone observations in the Western Mediterranean (Velchev et al., 2011). The Mediterranean is subject to episodes of import of UTLS ozone-enriched air through tropopause folds formed along the sub-tropical jet (Weigel et al., 2012), or due to the propensity for cut-off low formation in the region (Nieto et al., 2005). The region is also subject to conditions favouring enhanced photochemical activity, as well as the long-range import of air masses from other Northern Hemisphere regions of ozone precursor emission. The Mediterranean Basin is surrounded by densely populated land regions to the north, and is a major receptor of European pollution exported at low altitudes in summer (Stohl et al., 2002; Duncan and Bey, 2004; Duncan et al., 2008). The Eastern Mediterranean has been shown to exhibit a factor 1.5–2.2 enhancement in ozone during northerly flow from mainland Europe in summer compared with periods of flow from North Africa (Kourtidis et al., 2002). Gerasopoulos et al. (2006) showed that episodes of enhanced summertime ozone abundances observed at Crete in the Eastern Mediterranean were mainly driven by import of air masses from the main European continent. Hot, dry summer conditions, for example during summer 2003, can lead to extensive forest fires in Portugal, France, Spain and Italy, influencing trace gas and aerosol abundances over the Mediterranean Basin (Pace et al., 2005; Hodzic et al., 2007; Strada et al., 2012) Biogenic emissions in summer also impact the Mediterranean Basin (Liakakou et al., 2007), and may increase summertime daily ozone maxima in the region by 5 ppbv (Curci et al., 2009). Model estimates suggest that temperature increases may lead to increases in biogenic emissions in the region by $9 \pm 3 \% \, K^{-1}$ (Im et al., 2011). The Mediterranean mid and upper troposphere can be perturbed by long-range pollution import from Northern Europe, North America and Asia (Lelieveld et al., 2002). As described above, the Mediterranean summer troposphere can be strongly influenced by an upper tropospheric anti-cyclone centred over the Tibetan plateau, associated with the Asian summer monsoon (Rodwell and Hoskins, 2001; Roelofs et al., 2003). This can result in enhancements to ozone and precursor abundances in the Eastern Mediterranean upper troposphere due to import of air masses from the Asian boundary layer (Roelofs et al., 2003; Scheeren et al., 2003). The upper and mid troposphere over the Western Mediterranean is influenced by import in large-scale westerly flow and adiabatic descent in summer (Rodwell and Hoskins, 1996, 2001).

Understanding the variability in Mediterranean tropospheric ozone and contributions from different sources is critical for prediction of future European air quality and climate. A recent modelling study suggested that ozone mixing ratios in regions of the Eastern Mediterranean increase almost linearly with increases in ambient temperatures by

1.0 ± 0.1 ppb O_3 K^{-1} (Im et al., 2011). Some long-term in-situ observations of ozone are available at the surface in this region, however in-situ observations are lacking over the non-coastal basin area and through the tropospheric column where, as described above, a complex mixture of source origins may control ozone abundance. Here, we exploit 4 yr of remotely-sensed tropospheric ozone profile observations from the NASA Tropospheric Emissions Spectrometer (TES) satellite instrument (Beer et al., 2001) and 2 yr of lower tropospheric ozone observations from the GOME-2 satellite instrument to examine the structure of ozone features over the Mediterranean basin in summer (JJA), and use a global chemical transport model investigate their sensitivities to global emission sources, and their radiative impacts in the Mediterranean region.

We describe the TOMCAT chemical transport model in Sect. 2. Section 3 describes the TES and GOME-2 observations along with the available surface observations, and we discuss the structure of the Mediterranean summertime ozone maximum in the observations and model. Section 4 presents results from model ozone source sensitivity experiments and sensitivities to different processes. Radiative impacts of Mediterranean summertime ozone are discussed in Sect. 5, with radiative contributions assigned to source regions, and conclusions are drawn in Sect. 6.

2 The TOMCAT 3-D model

We use the TOMCAT 3-dimensional global chemical transport model (Arnold et al., 2005; Chipperfield, 2006) to simulate global tropospheric ozone, and calculate sensitivities of Mediterranean tropospheric ozone to different emission sources of ozone precursors. Simulations are performed at $\sim 2.8° \times 2.8°$ horizontal resolution, with 31 hybrid sigma-pressure levels in the vertical extending from the surface to 10 hPa and the model is forced using ECMWF ERA-Interim temperature, winds and humidity. Sub-grid transport from convection (Stockwell and Chipperfield, 1999). The non-local boundary layer scheme of Holtslag and Boville (1993) has been implemented in this version of TOMCAT (Wang et al., 1999), the scheme has been shown to perform well in comparisons to other models and to a version of TOMCAT using the local Louis (1979) scheme in Hoyle et al. (2011). This study uses a newly extended VOC degradation chemistry scheme, which incorporates the oxidation of monoterpenes based on the MOZART-3 scheme (Kinnison et al., 2007) and the oxidation of C2–C4 alkanes, toluene, ethane, propene, acetone, methanol and acetaldehyde based on the ExTC (Extended Tropospheric Chemistry) scheme (Folberth et al., 2006). The implementation of this scheme into TOMCAT is described by Monks (2011). Isoprene oxidation follows the Mainz Isoprene Mechanism I (Pöschl et al., 2000). Heterogeneous N_2O_5 hydrolysis is included using offline size-resolved aerosol from the GLOMAP model

(Mann et al., 2010). Uptake coefficients for different aerosol types are as parameterized by Evans and Jacob (2005), with the exception of dust which is based on Mogili et al. (2006). Anthropogenic emissions are taken from IPCC AR5 2000 emissions set (Lamarque et al., 2010). Biomass burning and natural wildfire emissions are prescribed from yearly varying monthly mean estimates from the Global Fire Emissions Database (GFED) v. 2 (van der Werf et al., 2006; Randerson et al., 2007). Natural isoprene and monoterpene emissions were calculated by the Model of Emissions of Gases and Aerosols from Nature (MEGAN) as implemented by Emmons et al. (2010). Other natural emissions are prescribed offline from the POET dataset (Granier et al., 2005). Dry deposition is determined using diurnally and seasonally varying surface-type specific deposition velocities, weighted by prescribed monthly land-cover fields from the NCAR community land model (Oleson et al., 2010).

3 Results and discussion

3.1 Evaluation of TOMCAT using surface observations

Surface observations were obtained from the EMEP (European Monitoring and Evaluation Programme) network of observing stations (Fjæraa and Hjellbrekke, 2010). Four stations in the Mediterranean region were selected for comparison with TOMCAT: 2 stations in the central and eastern region where the highest summertime ozone concentrations are observed (IT01 in Italy and GR02 in Greece) and 2 stations in the west where summertime concentrations are lower (ES12 and ES14 in Spain), see Table 1. These four stations were chosen as they represent the only EMEP stations within Mediterranean basin that have sufficient data for the time period of this study (2005–2008). The TOMCAT model was run for years 2005 to 2008 inclusive. The model was output every 1.75 days in order to capture the mean diurnal ozone cycle and the surface level ozone for the model grid box containing each station was selected for comparison. The station data, which are collected hourly, were then time matched to the TOMCAT output times and monthly mean data were constructed for both datasets. The resulting comparisons are shown in Fig. 1. A pronounced summer maximum in surface ozone is evident in the stations over the central and eastern Mediterranean (IT01 and GR02), with the Italian station showing ozone concentrations as large as 80 ppbv, which are almost 4 times higher than the corresponding winter values. This peak is not present at the western stations over Spain (ES12 and ES14), where there is only a very small seasonal cycle in the observed surface ozone.

The model reproduces the seasonal cycle at the IT01 station, although it tends to underestimate the observed concentrations in all years, with a mean summertime bias of -17.6 ppbv (-24%). The comparison is better for the GR02 site, where the model is able to capture the magnitude of

Table 1. EMEP stations used for the comparisons to TOMCAT shown in Fig. 1.

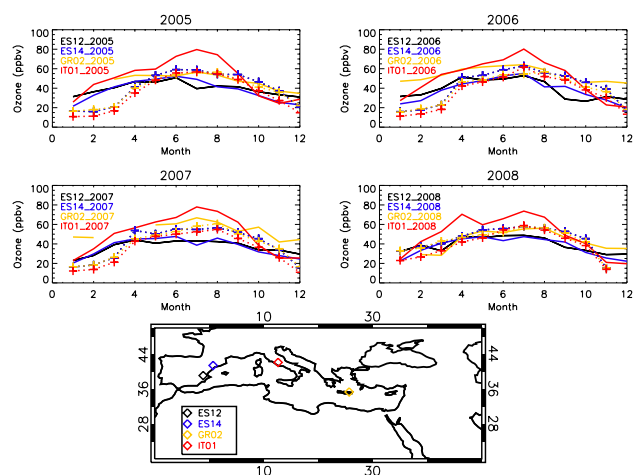| Code	Station name	Country	Latitude	Longitude	Altitude (m)
ES12	Zarra	Spain	39.08° N	1.1° W	885
ES14	Els Torms	Spain	41.4° N	0.72° E	470
GR02	Finokalia	Greece	35.32° N	25.67° E	0
IT01	Montelibretti	Italy	42.1° N	12.63° E	48

Fig. 1. Comparison of TOMCAT (dotted lines/symbols) and EMEP (solid lines) monthly mean surface ozone (ppbv) for the years 2005–2008. The different colours represent the different stations as depicted on the map in the lower panel, where ES12 = Zarra, ES14 = Els Torms, GRO2 = Finokalia and IT01 = Montelibretti.

the summertime peak (mean summertime bias of −2 ppbv (3.42 %)), although the model does tend to underestimate ozone concentrations in the winter and spring for all years except 2008 where the seasonal cycle is captured well. For the western stations (ES12 and ES14) the model exhibits a more pronounced seasonal cycle than seen in the observations, with a tendency to underestimate surface ozone in the winter and overestimate throughout the rest of the year, and has a mean summertime bias of 10.5 ppbv (24 %). One reason for this over/under estimation might be a combination of the resolution of the model which is relatively coarse (2.8° by 2.8°), resulting in model grid boxes containing the stations to extend eastwards over the Mediterranean, and therefore not being wholly representative of the conditions at these coastal sites.

3.2 Evaluation of TOMCAT using satellite observations

Comparisons with in-situ surface observations limit evaluation of the model to a limited set of locations at the surface. Satellite observations provide much better spatial coverage and give us the opportunity to evaluate the model over a large region and also with limited vertical information. In order to compare model output such as TOMCAT with remotely sensed satellite observations we must first take into account the limited vertical resolution and the effects of the a priori in the retrieved satellite profiles. Both of these effects are accounted for by applying the observation operator (averaging kernel and a priori information) for each retrieved satellite profile to the corresponding model profile before comparison. For both the TES and GOME-2 comparisons shown here we apply averaging kernels following the method of Rodgers and Connor (2003).

3.2.1 Comparisons with the Tropospheric Emission Spetrometer (TES)

The Tropospheric Emission Spectrometer (TES) is an infrared Fourier transform spectrometer which was launched onboard NASA's Aura satellite in 2004. The data used in this study comes from the TES Global Survey operating mode in which TES makes nadir observations with a 5.3×8.3 km footprint providing near global coverage approximately every 16 days. TES ozone profiles have been extensively vali-

dated against in-situ observations (Nassar et al., 2008; Osterman et al., 2008; Richards et al., 2008).

In order to compare TOMCAT with TES tropospheric ozone observations the model was run for the years 2005 to 2008 inclusive using the setup described in Sect. 2. In order to coincide with the TES overpass times the model was output at 12:00 UT and 00:00 UT during the months of June, July and August of each year. The TOMCAT profiles closest to each of the TES observations both spatially and temporally were selected for comparison. TES averaging kernels for each profile were then applied to the TOMCAT output. Both the resulting profiles and the TES data were then averaged onto the TOMCAT horizontal grid and summertime averages (JJA) were constructed for each year for comparison.

Figure 2 shows the comparison between TES and TOMCAT (with averaging kernels applied) at the 825 hPa level for the years 2005–2008 inclusive. The TES data clearly shows enhanced ozone concentrations over the whole of Mediterranean basin in all years, with concentrations of up to 110 ppbv observed in 2006. The highest ozone concentrations are seen in the southeastern coastal regions, along the north coasts of Libya and Egypt and into Israel. Large ozone concentrations (70–80 ppbv) are also observed over the industrialised northern regions of Greece and Italy, consistent with the surface observations described in Sect. 3.1. The TES data also shows that smaller ozone concentrations are present over the western Mediterranean region with values of ∼ 40 ppbv observed over Spain, which is again consistent with the surface observations.

TOMCAT and TES observations show general agreement in each of the years with correlations of between $r = 0.52$ and $r = 0.76$, and the model is able to capture the spatial
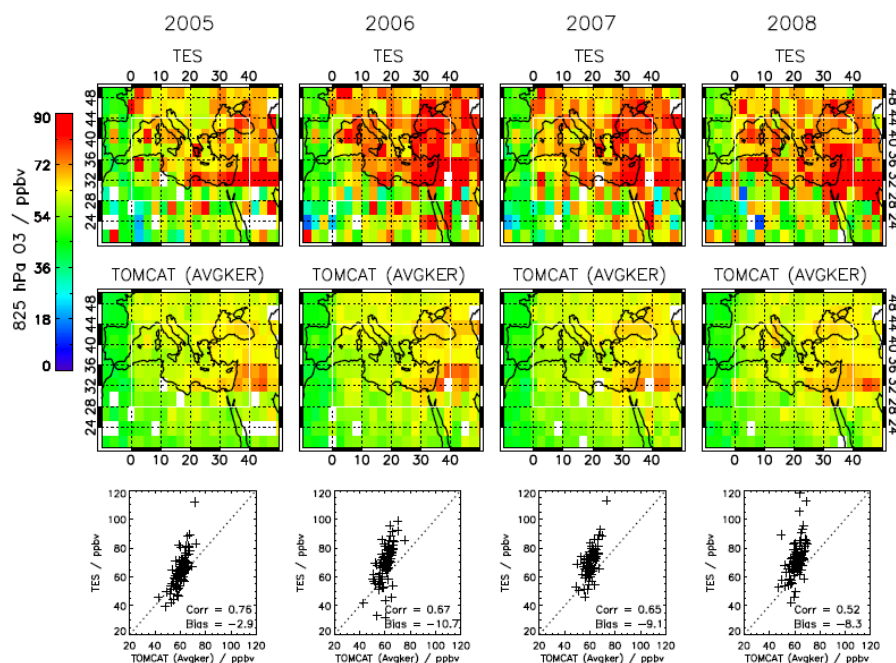
Fig. 2. Comparison of TES (top panels) and TOMCAT (middle panels) 825 hPa summertime ozone (ppbv) over the Mediterranean region for the years 2005–2008 inclusive. The TOMCAT model output has been matched in time and space to each TES observation and the TES averaging kernels have been applied before both sets of data have then been averaged over the months of June, July and August. The bottom panels show the correlation between the two datasets within the white box shown in the top two panels.

pattern of the observed ozone in the Mediterranean (the white boxes in Fig. 2). The model reproduces observed enhancements in ozone over Italy, Greece and the southeast of the region, also the smaller ozone concentrations observed over the west and Spain are well captured. Although the model compares well to TES in terms of the spatial pattern of the ozone distribution, it exhibits a median low bias of between -2.9 ppbv (4.5 %) and -10.7 ppbv (-13.8 %) across the 4 yr when compared to TES. The apparent low bias seen in TOMCAT when compared to TES is similar to that shown in the GEOS-Chem model compared with TES ozone over the Mediterranean basin (Liu et al., 2009). Validation of TES ozone profiles against LIDAR observations showed that TES may have a high bias in near-surface ozone of up to 15 % (Richards et al., 2008), possibly accounting for the biases observed here. This is also supported by the fact that TOMCAT shows a much smaller fractional bias against GOME-2 0–6 km ozone column measurements, as discussed in the next section.

3.2.2 Comparisons with the Global Ozone Monitoring Experiment-2 (GOME-2)

The ESA GOME-2 instrument is a nadir-viewing spectrometer with spectral coverage from 240–790 nm aboard the MetOp-A satellite platform (Riese et al., 2012). GOME-2 measures backscattered radiance from the Earth's atmo-

sphere in addition to a solar reference measurement. The instrument has a nominal ground footprint of 40 km × 80 km with global coverage in a day. For the scheme applied here, the ground pixels have been combined to create pixels 160 km × 160 km in order to improve signal-to-noise while not introducing significant inaccuracy from scene inhomogeneity. The Rutherford Appleton Laboratory (RAL) GOME-2 ozone profile product has been developed from the scheme applied to GOME-1 (Munro et al., 1998; Forster et al., 2007a) aboard ERS-2, which demonstrated the capability to discern tropospheric ozone using the Huggins ozone bands. The RAL GOME-2 scheme is in the process of validation. The bias and SD with respect to ozonesondes in the region studied in this paper are 2 and 5 DU, respectively, for the 0–6 km sub column (Hodzic et al., 2007).

Figure 3 shows comparisons of GOME-2 and TOMCAT for the years 2007 and 2008. The GOME-2 data shows a clear enhancement in ozone over the Mediterranean basin in both years. The largest ozone concentrations are observed over the eastern Mediterranean region with ozone values up to 40 DU in the 0–6 km column (corresponding to approximately 85 ppbv for the 0–6 km average). Large ozone concentrations (> 30 DU) are also observed over the central Mediterranean in the region of Italy and Greece. Smaller ozone concentrations (< 20 DU) are observed over western Mediterranean countries such as Spain. These observations are consistent with the spatial distribution of ozone observed
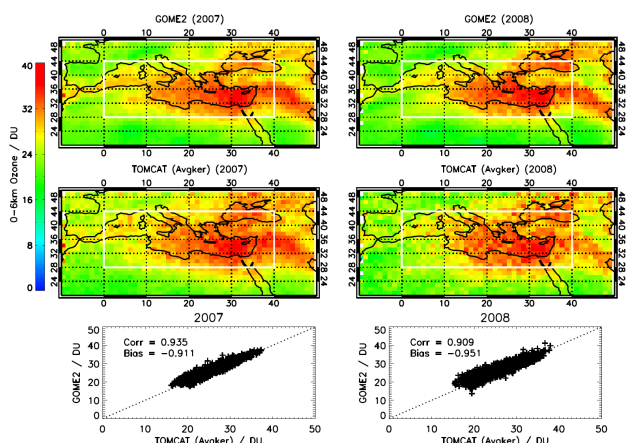
Fig. 3. Comparison of GOME-2 (top panels) and TOMCAT (middle panels) 0–6 km sub-column summertime ozone (DU) over the Mediterranean region for the years 2007 (left) and 2008 (right). The TOMCAT model output has been matched in time (within 6 h) and space to each GOME-2 observation and the GOME-2 averaging kernels have been applied before both sets of data have then been averaged over the months of June, July and August. The bottom panels show the correlation between the model and satellite observations for points within the white box shown in the top four panels.

Fig. 4. Map showing the region of interest in this study. The red box depicts what is referred to as the Mediterranean region, and the blue box shows the region referred to as "local" for the purposes of the emissions reductions applied in the model sensitivity experiments.

by both TES and surface sites. TOMCAT is able to capture the spatial distribution of ozone over the region as observed by GOME-2, with correlations of $r = 0.935$ and $r = 0.909$ for the years 2007 and 2008, respectively. The results also show that TOMCAT performs well in reproducing the GOME-2 observed concentrations and shows only a small bias of $< -1\,\text{DU}$ ($< 3\,\%$), which is within the precision of GOME-2 when compared to ozonesonde measurements.

4 Sensitivities of Mediterranean summertime ozone to emission sources

To determine sensitivities of the summertime Mediterranean ozone maximum to different local and remote sources, we have performed a series of TOMCAT model experiments. These consist of a base run with standard emissions (as described in Sect. 2) and eight sensitivity runs, each with a 20 % reduction in different local and global ozone precursor emission sources, detailed in Table 2. Emission reductions of 20 % are large enough to produce small perturbations to modelled ozone, and are small enough such that their impacts on ozone can be approximately linearly scaled to give expected results from emissions changes that may reasonably arise through legislation (e.g. 10–60 %) (Wild et al., 2012). Here, the term "local" encompasses the Mediterranean, Western and Eastern Europe and North Africa, denoted by the blue box shown in Fig. 4. Global emissions reductions also include the reductions in this region. The sim-
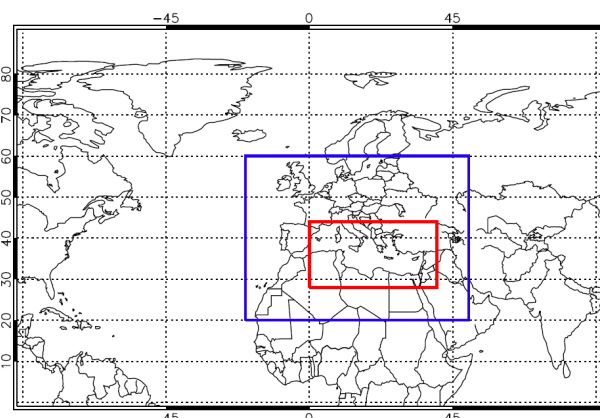
ulations were initialised in January 2006 and output is analysed for the summer months (JJA). These were compared to the base run in order to assess the impact of the different sources to summertime ozone in the region.

4.1 Sensitivities to local sources

Figure 5 shows the reduction in surface level, zonal-mean and meridional-mean ozone concentrations for the four experiments in which local emissions were reduced. The mean surface ozone reductions over the Mediterranean region for each experiment are also presented in Table 2.

4.1.1 Biomass burning

Local biomass burning emissions have little impact on ozone at all altitudes over the entire Mediterranean region, with a 20 % cut in emissions leading to a mean change in surface ozone concentrations of only 0.15 ppbv. The changes are slightly larger in the west of the region (0.19 ppbv for longitudes between 0° and 20° E) than in the east (0.11 ppbv for longitudes between 20° and 40° E). The GFED fire emissions for this region and period show largest emissions in Portugal and NW Spain, which explains the dominance of these emissions perturbations on the Western basin. Overall, the total NO_x emissions from fires in the Mediterranean region are approximately a factor 70 smaller than anthropogenic emissions, resulting in the smaller ozone perturbations due to fire emissions.

4.1.2 Anthropogenic VOCs

Local anthropogenic VOC emissions have only a small impact on ozone in the region with an average reduction in near-surface ozone of less than 0.15 ppbv for a 20 % cut in emissions. This reflects a strongly NO_x-limited ozone production

Table 2. TOMCAT sensitivity experiments performed to investigate the effect of reducing certain emissions sources by 20 %.

Run name	Emission type	Species	Mean surface ozone reduction (ppbv)	Top of the atmosphere mean radiative effect (mW m^{-2})
LBVOC	Local biogenic VOCs	$C_{10}H_{16}$, Methanol, Acetone, Isoprene	0.96	−3.5
LVOC	Local anthropogenic VOCs	Butanes, C_2H_6, C_3H_8, Aromatics, Acetone, C_2H_2, C_2H_4, Methanol, C_3H_6	0.15	−1.1
LNOX	Local anthropogenic NO$_x$	NO$_x$	2.09	−9.6
LBB	Local biomass burning	All biomass burning species	0.15	−2.0
AAN	All Asian anthropogenic and natural	All Asian emissions	0.46	−38.3
NAM	All North American anthropogenic and natural	All North American Emissions	0.94	−18.2
GVOC	Global anthropogenic VOCs	Butanes, C_2H_6, C_3H_8, Aromatics, Acetone, C_2H_2, C_2H_4, Methanol, C_3H_6	0.25	−5.3
GBVOC	Global biogenic VOCs	$C_{10}H_{16}$, Methanol, Acetone, Isoprene	1.66	−33.1
GNOX	Global anthropogenic NO$_x$	NO$_x$	2.49	−33.3

regime in the global model, characteristic of a dominance of rural areas as a source of ozone on the regional scale where NO$_x$ concentrations are relatively low compared with highly concentrated NO$_x$-saturated urban plumes (Jacob et al., 1993). The modelled ozone changes are fairly homogeneous throughout the Mediterranean basin. The largest ozone changes are seen near the surface and decrease with increasing altitude down to 0.08 ppbv at 700 hPa, and less than 0.03 ppbv at altitudes above the 700 hPa level. The lack of strong vertical transport over the Mediterranean in summer, suppressed by the dominant anticyclonic conditions discussed in the Introduction, lead to the effects of local emissions on Mediterranean ozone being largely confined to the surface boundary layer.

4.1.3 Biogenic VOCs

Local biogenic VOC emissions have a more significant effect on ozone in the region. A 20 % cut in local biogenic VOC emissions leads to widespread reductions in ozone over the Mediterranean, with an average reduction of 0.96 ppbv near the surface. Larger changes are seen in the north and east of the region (1.05 ppbv) compared to the west (0.87 ppbv). The ozone reductions are largest in the boundary layer and are

confined to the lower troposphere, with ozone changes dropping to 0.55 ppbv at 700 hPa. At altitudes above the 700 hPa level the changes in ozone reduce with altitude to 0.12 ppbv at 500 hPa. The more significant impact of biogenic emissions on ozone compared with anthropogenic emissions reflects the high reactivity of isoprene and the resulting efficient radical source in the rural atmosphere. In addition, an important mechanism is the role of isoprene in regional PAN formation, which sustains NO$_x$ abundances and ozone production remote from NO$_x$ emission regions. The model predicts that perturbations to regional PAN concentrations are an order of magnitude larger with a perturbation to biogenic emissions compared with local anthropogenic VOC or biomass burning emissions.

4.1.4 Anthropogenic NO$_x$

Of all of the precursor emissions considered, local NO$_x$ emissions have the largest impact on ozone in the Mediterranean, again reflecting the strong NO$_x$-limitation of the model ozone production. A 20 % cut in local NO$_x$ emissions leads to a mean reduction in ozone over the region of 2.09 ppbv near the surface. The reduction in ozone is not, however, homogeneous, and in contrast to biogenic VOCs,
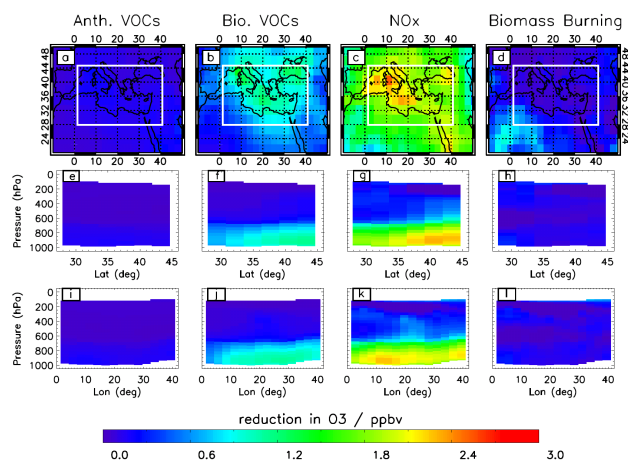
Fig. 5. Reduction in mean summertime (JJA) ozone (ppbv) resulting from a 20 % reduction in four local precursor species emissions (from left to right: anthropogenic VOC, biogenic VOC, NO$_x$ and biomass burning). The top row shows the reduction is surface level ozone over the Mediterranean region. The middle row shows zonal mean ozone reductions within the white boxes depicted in the maps on the top row. The bottom row shows meridional means of the ozone reduction, also within the white boxes. For zonal and meridional mean plots, only tropospheric model grid boxes are plotted (determined as where potential temperature < 380 K and PVU < 2).
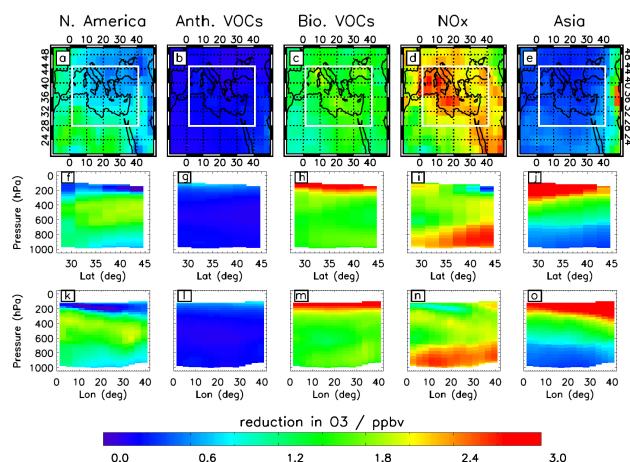
Fig. 6. Reduction in mean summertime (JJA) ozone (ppbv) resulting from a 20 % reduction in five global precursor species emissions (from left to right: North American emissions, anthropogenic VOC, biogenic VOC, NO$_x$ and Asian emissions). The top row shows the reduction in surface level ozone over the Mediterranean region. The middle row shows zonal mean ozone reductions within the white boxes depicted in the maps on the top row. The bottom row shows meridional means of the ozone reduction, also within the white boxes. For zonal and meridional mean plots, only tropospheric model grid boxes are plotted (determined as where potential temperature < 380 K and PVU < 2).

the largest changes are in the industrialised central and northwestern areas of the region, with the maximum change in ozone (2.45 ppbv) occurring off the west coast of Italy, close to Rome. As with the other local emission sources, the greatest changes in ozone from local NO$_x$ emissions are confined to the lower troposphere, with a sharp decrease at around 650 hPa.

4.2   Global sensitivities

Figure 6 shows the reduction in ozone simulated with 20 % reductions applied to global emissions, and individually to North American and Asian emissions. The mean surface ozone reductions over the Mediterranean region for each experiment are also presented in Table 2. It is important to note that the global emission reduction experiments also include the same cuts in local emissions as described in Sect. 4.1. In order to quantify the additional ozone sensitivity from the inclusion of cuts in "rest of world" emissions we have calculated the percentage global contribution to the ozone sensitivity as $100 \times (\Delta O_{3(\text{global})} - \Delta O_{3(\text{local})})/\Delta O_{3(\text{global})}$. The resulting surface, zonal and meridional distributions of "rest of world" percentage contribution to ozone sensitivities are shown in Fig. 7.

4.2.1   Anthropogenic VOCs

As with the local anthropogenic VOC emissions reduction, global anthropogenic VOCs have little effect on Mediter-

ranean ozone. For a 20 % cut in global emissions the mean reduction in near-surface ozone in the region is 0.25 ppbv. This reduction is uniform throughout the entire Mediterranean region. This change in ozone is also homogeneous in the vertical with similar changes in ozone seen at all levels up to 200 hPa. Above 200 hPa the modelled ozone change increases, reaching 0.69 ppbv at 100 hPa. This is in contrast to the changes seen for local emission cuts which were largest near the surface, indicating that long-range transport of VOCs, or ozone originating from remote VOC emissions, has a larger impact on ozone concentration in the upper troposphere than in the lower. The percentage global contribution to the modelled ozone changes due to global VOC emission cuts is 35 % at the surface (Fig. 7a). However, at altitudes above the 700 hPa level, global VOC emissions begin to dominate the sensitivity of ozone to anthropogenic VOC emission reductions, rising from 55 % at 700 hPa to over 80 % above the 500 hPa level (Fig. 7d and g).

4.2.2   Biogenic VOCs

Global biogenic VOC emissions have a widespread impact on near-surface Mediterranean ozone with mean reduction of 1.66 ppbv for a 20 % cut in emissions. Unlike local emissions, which have a larger impact in the north and east of the basin, global biogenic VOC emissions produce a near homogeneous change in ozone throughout the region. These changes in ozone also extend in the vertical throughout the

troposphere remaining at around 1.6 ppbv up to altitudes of 250 hPa. At this altitude there is a sharp increase in the change in ozone resulting from these sources, rising to 3.46 ppbv at 100 hPa. Again, this is in contrast to the effect of local emissions which were confined to the lower troposphere (below the 700 hPa level). The large impact of global biogenic emissions throughout the Mediterranean tropospheric profile is explained by the role of isoprene in controlling PAN formation and the global NO_y distribution. The model shows that under a 20 % reduction in global biogenic emissions, the formation of PAN and its transport to the mid-latitude middle and upper troposphere is reduced by between 20 and 30 %. This leads to reductions in NO_x over the Mediterranean at the surface of up to 5 % and at ~500 hPa of up to 8 %. The percentage global contribution to the ozone change shows that in the regions where the local emissions produced the largest changes (north and east) the global BVOC contribution is only around 30 %, whereas throughout the rest of the Mediterranean basin the contribution rises to 60 % (Fig. 7b). The global biogenic VOC contribution in the lower troposphere (below the 700 hPa level) is, on average, 47 %. At altitudes above the 700 hPa level, however, there is a sharp increase in this contribution, reaching 90 % at 500 hPa further increasing to > 99 % at 150 hPa.

4.2.3 Anthropogenic NO_x

Local NO_x emissions dominate near the surface, with the largest impact on ozone in the west of the region with widespread changes of up to 3.01 ppbv, compared to a maximum of 2.63 ppbv in the east. In the south of the region the maximum changes in ozone extend upwards to only around 800 hPa, whereas in the north the large changes in ozone continue up to around 600 hPa. Unlike the ozone changes seen with local NO_x emission cuts, large changes in ozone (~ 1.8 ppbv) still persist throughout the middle and upper troposphere (600–200 hPa) with a secondary peak of 1.94 ppbv present at around 150 hPa in the north and east. This reflects the altitudes of maximum influence from North American and Asian emission sources over the Mediterranean (see following sections). Global NO_x emissions account for only 15–20 % of the ozone changes in the lower troposphere (below 700 hPa). This contribution increases markedly at higher altitudes, and exhibits a north/south split. At around 600 hPa it reaches 90 % in the south, whereas in the north, it is only 50 % at this level, reaching 90 % at 300 hPa.

4.2.4 Asian emissions

Asian emissions have a moderate impact on near-surface ozone concentrations throughout the region, with a mean change in ozone of 0.46 ppbv for a 20 % cut in emissions. Of the emission sources considered here, this makes Asian emissions the fourth most important emission source for sur-
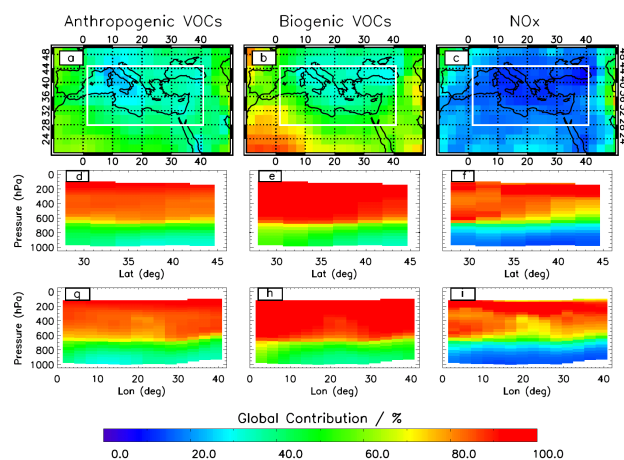

Fig. 7. Contribution of global emissions (%) to changes in mean summertime (JJA) ozone for three precursor species emissions (from left to right: anthropogenic VOC, biogenic VOC and NO_x). The top row shows the contributions to surface level ozone over the Mediterranean region. The middle row shows zonal means of the contribution within the white boxes depicted in the maps on the top row. The bottom row shows meridional means of the contribution, also within the white boxes. For zonal and meridional mean plots, only tropospheric model grid boxes are plotted (determined as where potential temperature < 380 K and PVU < 2).

face ozone sensitivity in the Mediterranean after local NO_x, local biogenic VOCs and emissions from North America. In contrast to local emissions, Asian emissions have a small impact on ozone concentrations in the lower troposphere (below 700 hPa). In the middle troposphere (700–400 hPa) the impact of Asian emissions is comparable to that of global biogenic VOC and NO_x emissions with mean ozone changes of 1.5 ppbv. However, it is in the upper troposphere where Asian emissions have their largest contribution to ozone, particularly in the north and east of the region, with ozone changes of up to 6.09 ppbv present at an altitude of 130 hPa. This is more than double the effect of global biogenic VOCs and triple that of global NO_x emissions. The large perturbation to upper tropospheric ozone is a result of efficient uplift of ozone precursors from South Asian emission sources in convection associated with the Asian monsoon. These air masses are carried into the upper troposphere over North Africa and into the Eastern Mediterranean in easterly flow associated with the upper-troposphere anti-cyclone discussed in the Introduction.

4.2.5 North American emissions

A 20 % cut North American emissions leads to a change in near-surface ozone concentrations throughout the Mediterranean region of 0.94 ppbv. This change in approximately equal to the ozone reduction seen for a 20 % cut in local biogenic VOC emissions. Of the sources considered here, this makes emissions from North America the third most

important emission source for near-surface ozone sensitivity in the Mediterranean after local NO_x and local biogenic VOCs. North American emissions have their greatest impact on ozone throughout the region in the mid to upper troposphere between 700 and 200 hPa, with a peak change in ozone of ~ 1.9 ppbv at 350 hPa in the west (longitudes $< 10°$ E) and ~ 2.0 ppbv at 600 hPa in the east (longitudes $> 30°$ E). However, unlike Asian and global emission sources, little or no changes in ozone are observed at altitudes above the 200 hPa level.

5 Radiative effects

The radiative effect caused by simulated changes in tropospheric ozone over the Mediterranean region under each emission reduction scenario was calculated using the offline version of the Edwards and Slingo (1996) radiative transfer model, with 6 bands in the shortwave, 9 bands in the longwave and a delta-Eddington 2 stream scattering solver at all wavelengths. A monthly averaged climatology of temperature, water vapour and trace gases based on the ECMWF reanalysis data, with $2.5° \times 2.5°$ horizontal resolution and 23 pressure levels in the vertical from the surface to 1 hPa was used (Rap et al., 2010). Cloud and surface albedo data were compiled from the International Satellite Cloud Climatology Project (ISCCP) archive (Rossow and Schiffer, 1999), averaged over the period from 1983 to 2005.

Figure 8 shows the JJA net radiative effect (RE) at the top-of-the-atmosphere (TOA) for the 9 different TOMCAT sensitivity experiments. The Mediterranean region TOA ozone RE means are -1.1 mW m^{-2}, -3.5 mW m^{-2}, -9.6 mW m^{-2}, and -2.0 mW m^{-2} for the local anthropogenic, biogenic, NO_x, and biomass burning experiments, respectively, and -5.3 mW m^{-2}, -18.2 mW m^{-2}, -33.1 mW m^{-2}, -33.3 mW m^{-2}, and -38.3 mW m^{-2} for the global anthropogenic, North American, biogenic, NO_x, and Asian experiments, respectively, see Table 2. Of all the precursor local emissions investigated here, reducing local NO_x has the largest ozone RE due to the fact that, as shown in Sect. 3.3.1, it has the largest impact on the ozone distribution. However, the REs for all four local experiments are relatively small, compared with the corresponding global experiments. This is caused on one hand by the larger ozone change in absolute numbers of the global experiments compared with the local ones, but, most importantly, also by the altitude at which these changes occur. At the latitudes of the Mediterranean region, the tropospheric ozone RE is most sensitive for ozone changes above 400 hPa, with a unit mass ozone change at 400 hPa and above resulting in a RE up to eight times as large as the RE induced by a similar change in ozone near the surface (Riese et al., 2012). Comparing two contrasting experiments from a RE perspective illustrates this point well, i.e. the local NO_x and the Asian experiments: although the local NO_x reduction has a larger impact on the
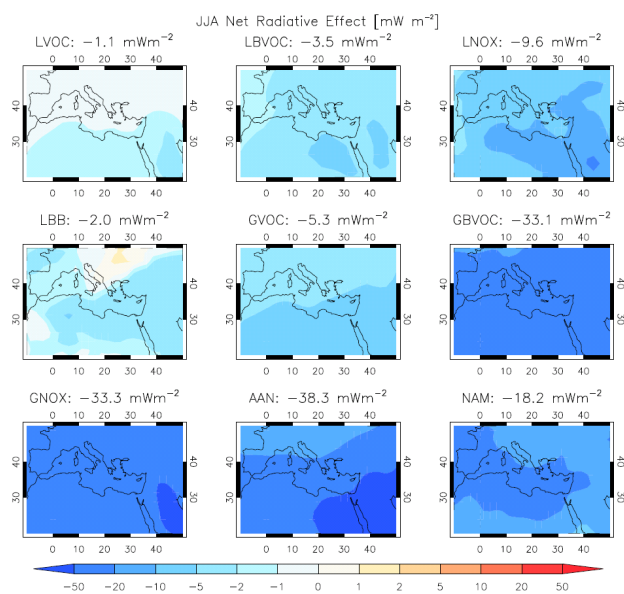

Fig. 8. Summertime (JJA) net (longwave + shortwave) radiative effects (in mW m^{-2}) over the Mediterranean region at the top-of-the-atmosphere (TOA) for the nine emission reduction experiments (see Table 2) compared to the "Base" reference run.

surface ozone distribution than the Asian emissions reduction (Fig. 5c compared with Fig. 6e), the ozone RE is substantially smaller in the former (-9.6 mW m^{-2}) compared with the latter (-38.3 mW m^{-2}) due to the difference in the upper tropospheric ozone perturbation between the two cases (Figs. 5g and 6j). Due to strong non-linearities in ozone production dependence on precursor abundance, it is not possible to linearly scale ozone changes resulting from fractional reductions in a precursor source to a 100 % total contribution from that source (e.g. Wild et al., 2012). However, a simple scaling suggests that the magnitude of the radiative effect on the Mediterranean climate due to ozone sourced from Asian emissions may be around half of the global mean tropospheric ozone radiative forcing since pre-industrial times (Forster et al., 2007a). This result has important implications for the effectiveness of European legislation aimed at controlling emissions of short-lived climate forcers and their precursors, in protecting Mediterranean climate.

6 Conclusions

We have used satellite observations and a state-of-the-art 3-D chemical transport model to investigate the structure of the Mediterranean summertime ozone maximum, and its sensitivities to regional and global emission sources. Both the TES and GOME-2 satellite instruments observe high ozone concentrations in the lower troposphere over the Mediterranean basin during summer, with the largest concentrations (up to 110 ppbv at 825 hPa) observed in the east. Comparisons of

the TOMCAT chemical transport model with EMEP surface observations, TES and GOME-2 show that TOMCAT is able to reproduce the observed summertime maximum in ozone over the Mediterranean region.

Model experiments were performed to determine the sensitivity of modelled summertime ozone over the Mediterranean region to different ozone precursor sources. These experiments show that lower tropospheric summertime ozone throughout the region has largest sensitivity to locally-emitted NO_x, particularly in the west. Biogenic VOCs produce the second largest sensitivity in summertime ozone in the Mediterranean to local sources, and have a stronger impact in the east of the region. Local sources have the greatest impact on ozone in the lower troposphere (below 700 hPa) with 80–85 % of the ozone sensitivity from NO_x resulting from local sources. Therefore, local sources of NO_x and biogenic VOCs are the most important factors in terms of controlling summertime ozone air quality in the Mediterranean. However, non-local sources have a larger effect on ozone in the upper troposphere, where it is much more radiatively inportant. This means that in terms of tropospheric ozone impacts on the local climate, Asian emissions, global NO_x, global biogenic VOC and North American emissions have a much larger impact than local emissions, with Asian emissions having a net radiative effect which is 4 times greater than that of local NO_x. Our model results support the picture of a layered structure vertically through the Mediterranean troposphere, with air masses influenced by different Northern Hemisphere source origins stacked vertically on top of one another (e.g. Lelieveld et al., 2002). Our results indicate that this layering, together with the increased radiative efficiency of ozone in the upper troposphere, means that remote sources in North America and Asia have a larger influence on ozone radiative forcing than local ozone precursor emissions, since their influence is greatest on ozone in the upper troposphere. Expected future increases in South Asian ozone precursor emissions (van Vuuren et al., 2011) could lead to increases in ozone climate forcing over the Mediterranean, despite projected aggressive reductions in local ozone precursor emissions.

Edited by: N. Mihalopoulos

References

Ancellet G., and Ravetta, F.: Analysis and validation of ozone variability observed by lidar during the ESCOMPTE-2001 campaign, Atmos. Res., 74, 435–459, doi:10.1016/j.atmosres.2004.10.003, 2005.

Arnold, S. R., Chipperfield, M. P., and Blitz, M. A.: A three-dimensional model study of the effect of new temperature-dependent quantum yields for acetone photolysis, J. Geophys. Res.-Atmos., 110, D22305 doi:10.1029/2005jd005998, 2005.

Beer, R., Glavich, T. A., and Rider, D. M.: Tropospheric emission spectrometer for the Earth Observing System's Aura Satellite, Appl. Optics, 40, 2356–2367, doi:10.1364/ao.40.002356, 2001.

Butkovic, V., Cvitas, T., and Klasinc, L.: Photochemical ozone in the Mediterranean, Sci. Total Environ., 99, 145–151, doi:10.1016/0048-9697(90)90219-k, 1990.

Castell, N., Mantilla, E., and Millan, M. M.: Analysis of tropospheric ozone concentration on a Western Mediterranean site: Castellon (Spain), Environ. Monit. Assess., 136, 3–11, doi:10.1007/s10661-007-9723-1, 2008.

Chipperfield, M. P.: New version of the TOMCAT/SLIMCAT offline chemical transport model: Intercomparison of stratospheric tracer experiments, Q. J. R. Meteorol. Soc., 132, 1179–1203, doi:10.1256/qj.05.51, 2006.

Collins, W. J., Sitch, S., and Boucher, O.: How vegetation impacts affect climate metrics for ozone precursors, J. Geophys. Res.-Atmos., 115, D23308 doi:10.1029/2010jd014187, 2010.

Curci, G., Beekmann, M., Vautard, R., Smiatek, G., Steinbrecher, R., Theloke, J., and Friedrich, R.: Modelling study of the impact of isoprene and terpene biogenic emissions on European ozone levels, Atmos. Environ., 43, 1444–1455, doi:10.1016/j.atmosenv.2008.02.070, 2009.

Duncan, B. N. and Bey, I.: A modeling study of the export pathways of pollution from Europe: Seasonal and interannual variations (1987–1997), J. Geophys. Res.-Atmos., 109, D08301, doi:10.1029/2003jd004079, 2004.

Duncan, B. N., West, J. J., Yoshida, Y., Fiore, A. M., and Ziemke, J. R.: The influence of European pollution on ozone in the Near East and northern Africa, Atmos. Chem. Phys., 8, 2267–2283, doi:10.5194/acp-8-2267-2008, 2008.

Edwards, J. M. and Slingo, A.: Studies with a flexible new radiation code .1. Choosing a configuration for a large-scale model, Q. J. Roy. Meteorol. Soc., 122, 689–719, doi:10.1256/smsqj.53106, 1996.

Emmons, L. K., Walters, S., Hess, P. G., Lamarque, J.-F., Pfister, G. G., Fillmore, D., Granier, C., Guenther, A., Kinnison, D., Laepple, T., Orlando, J., Tie, X., Tyndall, G., Wiedinmyer, C., Baughcum, S. L., and Kloster, S.: Description and evaluation of the Model for Ozone and Related chemical Tracers, version 4 (MOZART-4), Geosci. Model Dev., 3, 43–67, doi:10.5194/gmd-3-43-2010, 2010.

Evans, M. J. and Jacob, D. J.: Impact of new laboratory studies of N(2)O(5) hydrolysis on global model budgets of tropospheric nitrogen oxides, ozone, and OH, Geophys. Res. Lett., 32, L09813, doi:10.1029/2005gl022469, 2005.

Fjæraa, A. M. and Hjellbrekke, A.-G.: Ozone measurements 2008, EMEP/CCC-Report 2/2010, available at: http://www.nilu.no/projects/ccc/reports.html, 2010.

Folberth, G. A., Hauglustaine, D. A., Lathière, J., and Brocheton, F.: Interactive chemistry in the Laboratoire de Météorologie Dy-

namique general circulation model: model description and impact analysis of biogenic hydrocarbons on tropospheric chemistry, Atmos. Chem. Phys., 6, 2273–2319, doi:10.5194/acp-6-2273-2006, 2006.

Forster, P., Ramaswamy, V., Artaxo, P., Berntsen, T., Betts, R., Fahey, D. W., Haywood, J., Lean, J., Lowe, D. C., Myhre, G., Nganga, J., Prinn, R., Raga, G., Schulz, M., and Dorland, R. V.: Changes in Atmospheric Constituents and in Radiative Forcing, in: Climate Change 2007: The Physical Science Basis. Contribution of Working Group I to the Fourth Assessment Report of the Intergovernmental Panel on Climate Change, edited: Solomon, S., Qin, D., Manning, M., Chen, Z., Marquis, M., Averyt, K. B., Tignor, M., and Miller, H. L., Cambridge University Press, Cambridge, United Kingdom and New York, NY, USA, 2007a.

Forster, P. M., Bodeker, G., Schofield, R., Solomon, S., and Thompson, D.: Effects of ozone cooling in the tropical lower stratosphere and upper troposphere, Geophys. Res. Lett., 34, L23813, doi:10.1029/2007gl031994, 2007b.

Fuhrer, J.: Ozone risk for crops and pastures in present and future climates, Naturwissenschaften, 96, 173–194, doi:10.1007/s00114-008-0468-7, 2009.

Gangoiti, G., Millan, M. M., Salvador, R., and Mantilla, E.: Long-range transport and re-circulation of pollutants in the western Mediterranean during the project Regional Cycles of Air Pollution in the West-Central Mediterranean Area, Atmos. Environ., 35, 6267–6276, doi:10.1016/s1352-2310(01)00440-x, 2001.

Gerasopoulos, E., Kouvarakis, G., Vrekoussis, M., Donoussis, C., Mihalopoulos, N., and Kanakidou, M.: Photochemical ozone production in the eastern Mediterranean, Atmos. Environ., 40, 3057–3069, doi:10.1016/j.atmosenv.2005.12.061, 2006.

Granier, C., Lamarque, J. F., Mieville, A., Muller, J. F., Olivier, J., Orlando, J., Peters, J., Petron, G., Tyndall, G., and Wallens, S.: POET, a database of surface emissions of ozone precursors, available at: http://www.aero.jussieu.fr/projet/ACCENT/POET.php, 2005.

Gryparis, A., Forsberg, B., Katsouyanni, K., Analitis, A., Touloumi, G., Schwartz, J., Samoli, E., Medina, S., Anderson, H. R., Niciu, E. M., Wichmann, H. E., Kriz, B., Kosnik, M., Skorkovsky, J., Vonk, J. M., and Dortbudak, Z.: Acute effects of ozone on mortality from the "Air pollution and health: A European approach" project, Am. J. Respir. Crit. Care Med., 170, 1080–1087, doi:10.1164/rccm.200403-333OC, 2004.

Hauglustaine, D. A. and Brasseur, G. P.: Evolution of tropospheric ozone under anthropogenic activities and associated radiative forcing of climate, J. Geophys. Res.-Atmos., 106, 32337–32360, doi:10.1029/2001jd900175, 2001.

Hodzic, A., Madronich, S., Bohn, B., Massie, S., Menut, L., and Wiedinmyer, C.: Wildfire particulate matter in Europe during summer 2003: meso-scale modeling of smoke emissions, transport and radiative effects, Atmos. Chem. Phys., 7, 4043–4064, doi:10.5194/acp-7-4043-2007, 2007.

Hollaway, M. J., Arnold, S. R., Challinor, A. J., and Emberson, L. D.: Intercontinental trans-boundary contributions to ozone-induced crop yield losses in the Northern Hemisphere, Biogeosciences, 9, 271–292, doi:10.5194/bg-9-271-2012, 2012.

Holtslag, A. A. M., and Boville, B. A.: Local versus nonlocal boundary-layer diffusion in a global climate model, J. Clim., 6, 1825–1842, doi:10.1175/1520-0442(1993)006¡1825:lvnbld¿2.0.co;2, 1993.

Hoyle, C. R., Marécal, V., Russo, M. R., Allen, G., Arteta, J., Chemel, C., Chipperfield, M. P., D'Amato, F., Dessens, O., Feng, W., Hamilton, J. F., Harris, N. R. P., Hosking, J. S., Lewis, A. C., Morgenstern, O., Peter, T., Pyle, J. A., Reddmann, T., Richards, N. A. D., Telford, P. J., Tian, W., Viciani, S., Volz-Thomas, A., Wild, O., Yang, X., and Zeng, G.: Representation of tropical deep convection in atmospheric models – Part 2: Tracer transport, Atmos. Chem. Phys., 11, 8103–8131, doi:10.5194/acp-11-8103-2011, 2011.

Im, U., Markakis, K., Poupkou, A., Melas, D., Unal, A., Gerasopoulos, E., Daskalakis, N., Kindap, T., and Kanakidou, M.: The impact of temperature changes on summer time ozone and its precursors in the Eastern Mediterranean, Atmos. Chem. Phys., 11, 3847–3864, doi:10.5194/acp-11-3847-2011, 2011.

Ito, K., De Leon, S. F., and Lippmann, M.: Associations between ozone and daily mortality – Analysis and meta-analysis, Epidemiology, 16, 446–457, doi:10.1097/01.ede.0000165821.90114.7f, 2005.

Jacob, D. J., Logan, J. A., Gardner, G. M., Yevich, R. M., Spivakovsky, C. M., Wofsy, S. C., Sillman, S., and Prather, M. J.: Factors regulating ozone over the United Statesa nd its export to the global atmosphere, J. Geophys. Res., 98, 14817–14826, 1993.

Jimenez, P., Lelieveld, J., and Baldasano, J. M.: Multiscale modeling of air pollutants dynamics in the northwestern Mediterranean basin during a typical summertime episode, J. Geophys. Res.-Atmos., 111, D18306, doi:10.1029/2005jd006516, 2006.

Kalabokas, P. D. and Bartzis, J. G.: Photochemical air pollution characteristics at the station of the NCSR-Demokritos, during the MEDCAPHOT-TRACE campaign in Athens, Greece (20 August 20 September 1994), Atmos. Environ., 32, 2123–2139, doi:10.1016/s1352-2310(97)00423-8, 1998.

Kalabokas, P. D. and Repapis, C. C.: A climatological study of rural surface ozone in central Greece, Atmos. Chem. Phys., 4, 1139–1147, doi:10.5194/acp-4-1139-2004, 2004.

Kalabokas, P. D., Viras, L. G., Bartzis, J. G., and Repapis, C. C.: Mediterranean rural ozone characteristics around the urban area of Athens, Atmos. Environ., 34, 5199–5208, doi:10.1016/s1352-2310(00)00298-3, 2000.

Kalabokas, P. D., Volz-Thomas, A., Brioude, J., Thouret, V., Cammas, J.-P., and Repapis, C. C.: Vertical ozone measurements in the troposphere over the Eastern Mediterranean and comparison with Central Europe, Atmos. Chem. Phys., 7, 3783–3790, doi:10.5194/acp-7-3783-2007, 2007.

Kalabokas, P. D., Cammas, J.-P., Thouret, V., Volz-Thomas, A., Boulanger, D., and Repapis, C. C.: Examination of the atmospheric conditions associated with high and low summer ozone levels in the lower troposphere over the Eastern Mediterranean, Atmos. Chem. Phys. Discuss., 13, 2457–2491, doi:10.5194/acpd-13-2457-2013, 2013.

Kinnison, D. E., Brasseur, G. P., Walters, S., Garcia, R. R., Marsh, D. R., Sassi, F., Harvey, V. L., Randall, C. E., Emmons, L., Lamarque, J. F., Hess, P., Orlando, J. J., Tie, X. X., Randel, W., Pan, L. L., Gettelman, A., Granier, C., Diehl, T., Niemeier, U., and Simmons, A. J.: Sensitivity of chemical tracers to meteorological parameters in the MOZART-3 chemical transport model, J. Geophys. Res.-Atmos., 112, D20302, doi:10.1029/2006jd007879, 2007.

Kourtidis, K., Zerefos, C., Rapsomanikis, S., Simeonov, V., Balis, D., Perros, P. E., Thompson, A. M., Witte, J., Calpini, B., Sharobiem, W. M., Papayannis, A., Mihalopoulos, N., and Drakou, R.: Regional levels of ozone in the troposphere over eastern Mediterranean, J. Geophys. Res.-Atmos., 107, 8140, doi:10.1029/2000jd000140, 2002.

Kouvarakis, G., Tsigaridis, K., Kanakidou, M., and Mihalopoulos, N.: Temporal variations of surface regional background ozone over Crete Island in the southeast Mediterranean, J. Geophys. Res.-Atmos., 105, 4399–4407, doi:10.1029/1999jd900984, 2000.

Kouvarakis, G., Vrekoussis, M., Mihalopoulos, N., Kourtidis, K., Rappenglueck, B., Gerasopoulos, E., and Zerefos, C.: Spatial and temporal variability of tropospheric ozone (O-3) in the boundary layer above the Aegean Sea (eastern Mediterranean), J. Geophys. Res.-Atmos., 107, 8137, doi:10.1029/2000jd000081, 2002.

Lamarque, J.-F., Bond, T. C., Eyring, V., Granier, C., Heil, A., Klimont, Z., Lee, D., Liousse, C., Mieville, A., Owen, B., Schultz, M. G., Shindell, D., Smith, S. J., Stehfest, E., Van Aardenne, J., Cooper, O. R., Kainuma, M., Mahowald, N., McConnell, J. R., Naik, V., Riahi, K., and van Vuuren, D. P.: Historical (1850–2000) gridded anthropogenic and biomass burning emissions of reactive gases and aerosols: methodology and application, Atmos. Chem. Phys., 10, 7017–7039, doi:10.5194/acp-10-7017-2010, 2010.

Lelieveld, J. and Dentener, F. J.: What controls tropospheric ozone?, J. Geophys. Res.-Atmos., 105, 3531–3551, doi:10.1029/1999jd901011, 2000.

Lelieveld, J., Berresheim, H., Borrmann, S., Crutzen, P. J., Dentener, F. J., Fischer, H., Feichter, J., Flatau, P. J., Heland, J., Holzinger, R., Korrmann, R., Lawrence, M. G., Levin, Z., Markowicz, K. M., Mihalopoulos, N., Minikin, A., Ramanathan, V., de Reus, M., Roelofs, G. J., Scheeren, H. A., Sciare, J., Schlager, H., Schultz, M., Siegmund, P., Steil, B., Stephanou, E. G., Stier, P., Traub, M., Warneke, C., Williams, J., and Ziereis, H.: Global air pollution crossroads over the Mediterranean, Science, 298, 794–799, doi:10.1126/science.1075457, 2002.

Levy, J. I., Carrothers, T. J., Tuomisto, J. T., Hammitt, J. K., and Evans, J. S.: Assessing the public health benefits of reduced ozone concentrations, Environ. Health Perspect., 109, 1215–1226, doi:10.1289/ehp.011091215, 2001.

Liakakou, E., Vrekoussis, M., Bonsang, B., Donousis, C., Kanakidou, M., and Mihalopoulos, N.: Isoprene above the Eastern Mediterranean: Seasonal variation and contribution to the oxidation capacity of the atmosphere, Atmos. Environ., 41, 1002–1010, doi:10.1016/j.atmosenv.2006.09.034, 2007.

Liu, J. J., Jones, D. B. A., Worden, J. R., Noone, D., Parrington, M., and Kar, J.: Analysis of the summertime buildup of tropospheric ozone abundances over the Middle East and North Africa as observed by the Tropospheric Emission Spectrometer Instrument (vol 114, D05304, 2009), J. Geophys. Res.-Atmos., 114, D07399, doi:10.1029/2009jd012045, 2009.

Louis, J. F.: Parametric model of vertical eddy fluxes in the atmosphere, Bound.-Lay. Meteorol., 17, 187–202, doi:10.1007/bf00117978, 1979.

Mann, G. W., Carslaw, K. S., Spracklen, D. V., Ridley, D. A., Manktelow, P. T., Chipperfield, M. P., Pickering, S. J., and Johnson, C. E.: Description and evaluation of GLOMAP-mode: a modal global aerosol microphysics model for the UKCA composition-climate model, Geosci. Model Dev., 3, 519–551, doi:10.5194/gmd-3-519-2010, 2010.

Millan, M. M., Salvador, R., Mantilla, E., and Kallos, G.: Photooxidant dynamics in the Mediterranean basin in summer: Results from European research projects, J. Geophys. Res.-Atmos., 102, 8811–8823, doi:10.1029/96jd03610, 1997.

Millan, M. M., Mantilla, E., Salvador, R., Carratala, A., Sanz, M. J., Alonso, L., Gangoiti, G., and Navazo, M.: Ozone cycles in the western Mediterranean basin: Interpretation of monitoring data in complex coastal terrain, J. Appl. Meteorol., 39, 487–508, doi:10.1175/1520-0450(2000)039¡0487:ocitwm¿2.0.co;2, 2000.

Millan, M. M., Sanz, M. J., Salvador, R., and Mantilla, E.: Atmospheric dynamics and ozone cycles related to nitrogen deposition in the western Mediterranean, Environ. Pollut., 118, 167–186, doi:10.1016/s0269-7491(01)00311-6, 2002.

Mogili, P. K., Kleiber, P. D., Young, M. A., and Grassian, V. H.: N2O5 hydrolysis on the components of mineral dust and sea salt aerosol: Comparison study in an environmental aerosol reaction chamber, Atmos. Environ., 40, 7401–7408, doi:10.1016/j.atmosenv.2006.06.048, 2006.

Monks, S. A.: A model study of chemistry and transport in the Arctic troposphere, PhD thesis, School of Earth and Environment, University of Leeds, 230 pp., 2011.

Munro, R., Siddans, R., Reburn, W. J., and Kerridge, B. J.: Direct measurement of tropospheric ozone distributions from space, Nature, 392, 168–171, doi:10.1038/32392, 1998.

Nassar, R., Logan, J. A., Worden, H. M., Megretskaia, I. A., Bowman, K. W., Osterman, G. B., Thompson, A. M., Tarasick, D. W., Austin, S., Claude, H., Dubey, M. K., Hocking, W. K., Johnson, B. J., Joseph, E., Merrill, J., Morris, G. A., Newchurch, M., Oltmans, S. J., Posny, F., Schmidlin, F. J., Vomel, H., Whiteman, D. N., and Witte, J. C.: Validation of Tropospheric Emission Spectrometer (TES) nadir ozone profiles using ozonesonde measurements, J. Geophys. Res.-Atmos., 113, D15s17, doi:10.1029/2007jd008819, 2008.

Nieto, R., Gimeno, L., De La Torre, L., Ribera, P., Gallego, D., Garcia-Herrera, R., Garcia, J. A., Nunez, M., Redano, A., and Lorente, J.: Climatological features of cutoff low systems in the Northern Hemisphere, J. Clim., 18, 3085–3103, doi:10.1175/jcli3386.1, 2005.

Nolle, M., Ellul, R., Heinrich, G., and Gusten, H.: A long-term study of background ozone concentrations in the central Mediterranean – diurnal and seasonal variations on the island of Gozo, Atmos. Environ., 36, 1391–1402, doi:10.1016/s1352-2310(01)00505-2, 2002.

Oleson, K. W., Lawrence, D. M., Bonan, G. B., Flanner, M. G., Kluzek, E., Lawrence, P. J., Levis, S., Swenson, S. C., Thornton, P. E., Dai, A., Decker, M., Dickinson, R., Feddema, J., Heald, C. L., Hoffman, F., Lamarque, J.-F., Mahowald, N., Niu, G.-Y., Qian, T., Randerson, J., Running, S., Sakaguchi, K., Slater, A., Stockli, R., Wang, A., Yang, Z.-L., Zeng, X., and Zeng, X.: Technical Description of version 4.0 of the Community Land Model (CLM). NCAR Technical Note NCAR/TN-478+STR, National Center for Atmospheric Research, Boulder, CO, 2010.

Osterman, G. B., Kulawik, S. S., Worden, H. M., Richards, N. A. D., Fisher, B. M., Eldering, A., Shephard, M. W., Froidevaux, L., Labow, G., Luo, M., Herman, R. L., Bowman, K. W., and Thompson, A. M.: Validation of Tropospheric Emission Spectrometer (TES) measurements of the total, stratospheric, and tro-

pospheric column abundance of ozone, J. Geophys. Res.-Atmos., 113, D15s16, doi:10.1029/2007jd008801, 2008.

Pace, G., Meloni, D., and di Sarra, A.: Forest fire aerosol over the Mediterranean basin during summer 2003, J. Geophys. Res.-Atmos., 110, D21202, doi:10.1029/2005jd005986, 2005.

Paoletti, E.: Impact of ozone on Mediterranean forests: A review, Environ. Pollut., 144, 463–474, doi:10.1016/j.envpol.2005.12.051, 2006.

Pöschl, U., von Kuhlmann, R., Poisson, N., and Crutzen, P. J.: Development and intercomparison of condensed isoprene oxidation mechanisms for global atmospheric modeling, J. Atmos. Chem., 37, 29–52, doi:10.1023/a:1006391009798, 2000.

Global Fire Emissions Database, Version 2 (GFEDv2.1), Data set, available at: http://daac.ornl.gov/ from Oak Ridge National Laboratory Distributed Active Archive Center, Oak Ridge, Tennessee, USA, 2007.

Randerson, J. T., van der Werf, G. R., Giglio, L., Collatz, G. J., and Kasibhatla, P. S.: Global Fire Emissions Database, Version 2 (GFEDv2.1), data set, available at: http://daac.ornl.gov/ from Oak Ridge National Laboratory Distributed Active Archive Center, Oak Ridge, Tennessee, USA, doi:10.3334/ORNLDAAC/849, 2007.

Rap, A., Forster, P. M., Jones, A., Boucher, O., Haywood, J. M., Bellouin, N., and De Leon, R. R.: Parameterization of contrails in the UK Met Office Climate Model, J. Geophys. Res.-Atmos., 115, D10205, doi:10.1029/2009jd012443, 2010.

Ravetta, F., Ancellet, G., Colette, A., and Schlager, H.: Long-range transport and tropospheric ozone variability in the western Mediterranean region during the Intercontinental Transport of Ozone and Precursors (ITOP-2004) campaign, J. Geophys. Res.-Atmos., 112, D10s46, doi:10.1029/2006jd007724, 2007.

Richards, N. A. D., Osterman, G. B., Browell, E. V., Hair, J. W., Avery, M., and Li, Q.: Validation of Tropospheric Emission Spectrometer ozone profiles with aircraft observations during the intercontinental chemical transport experiment-B, J. Geophys. Res.-Atmos., 113, D16s29, doi:10.1029/2007jd008815, 2008.

Riese, M., Ploeger, F., Rap, A., Vogel, B., Konopka, P., Dameris, M., and Forster, P.: Impact of uncertainties in atmospheric mixing on simulated UTLS composition and related radiative effects, J. Geophys. Res.-Atmos., 117, D16305, doi:10.1029/2012jd017751, 2012.

Rodgers, C. D. and Connor, B. J.: Intercomparison of remote sounding instruments, J. Geophys. Res.-Atmos., 108, 4116, doi:10.1029/2002jd002299, 2003.

Rodwell, M. J. and Hoskins, B. J.: Monsoons and the dynamics of deserts, Q. J. R. Meteorol. Soc., 122, 1385–1404, doi:10.1002/qj.49712253408, 1996.

Rodwell, M. J. and Hoskins, B. J.: Subtropical anticyclones and summer monsoons, J. Clim., 14, 3192–3211, doi:10.1175/1520-0442(2001)014¡3192:saasm¿2.0.co;2, 2001.

Roelofs, G. J., Scheeren, H. A., Heland, J., Ziereis, H., and Lelieveld, J.: A model study of ozone in the eastern Mediterranean free troposphere during MINOS (August 2001), Atmos. Chem. Phys., 3, 1199–1210, doi:10.5194/acp-3-1199-2003, 2003.

Rossow, W. B. and Schiffer, R. A.: Advances in understanding clouds from ISCCP, B. Am. Meteorol. Soc., 80, 2261–2287, doi:10.1175/1520-0477(1999)080¡2261:aiucfi¿2.0.co;2, 1999.

Sauvage, B., Martin, R. V., van Donkelaar, A., Liu, X., Chance, K., Jaeglé, L., Palmer, P. I., Wu, S., and Fu, T.-M.: Remote sensed and in situ constraints on processes affecting tropical tropospheric ozone, Atmos. Chem. Phys., 7, 815–838, doi:10.5194/acp-7-815-2007, 2007.

Scheeren, H. A., Lelieveld, J., Roelofs, G. J., Williams, J., Fischer, H., de Reus, M., de Gouw, J. A., Warneke, C., Holzinger, R., Schlager, H., Klüpfel, T., Bolder, M., van der Veen, C., and Lawrence, M.: The impact of monsoon outflow from India and Southeast Asia in the upper troposphere over the eastern Mediterranean, Atmos. Chem. Phys., 3, 1589–1608, doi:10.5194/acp-3-1589-2003, 2003.

Sitch, S., Cox, P. M., Collins, W. J., and Huntingford, C.: Indirect radiative forcing of climate change through ozone effects on the land-carbon sink, Nature, 448, 791–794, doi:10.1038/nature06059, 2007.

Staehelin, J., Thudium, J., Buehler, R., Volzthomas, A., and Graber, W.: Trends in surface ozone concentrations at Arosa (Switzerland), Atmos. Environ., 28, 75–87, doi:10.1016/1352-2310(94)90024-8, 1994.

Stockwell, D. Z. and Chipperfield, M. P.: A tropospheric chemical-transport model: Development and validation of the model transport schemes, Q. J. Roy. Meteorol. Soc., 125, 1747–1783, doi:10.1256/smsqj.55713, 1999.

Stohl, A., Eckhardt, S., Forster, C., James, P., and Spichtinger, N.: On the pathways and timescales of intercontinental air pollution transport, J. Geophys. Res.-Atmos., 107, 4684, doi:10.1029/2001jd001396, 2002.

Strada, S., Mari, C., Filippi, J. B., and Bosseur, F.: Wildfire and the atmosphere: Modelling the chemical and dynamic interactions at the regional scale, Atmos. Environ., 51, 234–249, doi:10.1016/j.atmosenv.2012.01.023, 2012.

van der Werf, G. R., Randerson, J. T., Giglio, L., Collatz, G. J., Kasibhatla, P. S., and Arellano Jr., A. F.: Interannual variability in global biomass burning emissions from 1997 to 2004, Atmos. Chem. Phys., 6, 3423–3441, doi:10.5194/acp-6-3423-2006, 2006.

Van Dingenen, R., Dentener, F. J., Raes, F., Krol, M. C., Emberson, L., and Cofala, J.: The global impact of ozone on agricultural crop yields under current and future air quality legislation, Atmos. Environ., 43, 604–618, doi:10.1016/j.atmosenv.2008.10.033, 2009.

van Vuuren, D. P., Bouwman, L. F., Smith, S. J., and Dentener, F.: Global projections for anthropogenic reactive nitrogen emissions to the atmosphere: an assessment of scenarios in the scientific literature, Curr. Opin. Environ. Sustain., 3, 359–369, doi:10.1016/j.cosust.2011.08.014, 2011.

Varotsos, C. A. and Cracknell, A. P.: Ozone depletion over greece as deduced from NIMBUS-7 Toms measurements, Int. J. Remote Sens., 14, 2053–2059, 1993.

Velchev, K., Cavalli, F., Hjorth, J., Marmer, E., Vignati, E., Dentener, F., and Raes, F.: Ozone over the Western Mediterranean Sea – results from two years of shipborne measurements, Atmos. Chem. Phys., 11, 675–688, doi:10.5194/acp-11-675-2011, 2011.

Volz, A., and Kley, D.: Evaluation of the montsouris series of ozone measurements made in the 19th-century, Nature, 332, 240–242, doi:10.1038/332240a0, 1988.

Wang, K. Y., Pyle, J. A., Sanderson, M. G., and Bridgeman, C.: Implementation of a convective atmospheric boundary layer scheme

in a tropospheric chemistry transport model, J. Geophys. Res.-Atmos., 104, 23729–23745, doi:10.1029/1999jd900383, 1999.

Weigel, K., Hoffmann, L., Günther, G., Khosrawi, F., Olschewski, F., Preusse, P., Spang, R., Stroh, F., and Riese, M.: A stratospheric intrusion at the subtropical jet over the Mediterranean Sea: air-borne remote sensing observations and model results, Atmos. Chem. Phys., 12, 8423–8438, doi:10.5194/acp-12-8423-2012, 2012.

Wild, O., Fiore, A. M., Shindell, D. T., Doherty, R. M., Collins, W. J., Dentener, F. J., Schultz, M. G., Gong, S., MacKenzie, I. A., Zeng, G., Hess, P., Duncan, B. N., Bergmann, D. J., Szopa, S., Jonson, J. E., Keating, T. J., and Zuber, A.: Modelling future changes in surface ozone: a parameterized approach, Atmos. Chem. Phys., 12, 2037–2054, doi:10.5194/acp-12-2037-2012, 2012.